Two-Flux Method for Transient Thermal Analysis in a Layer of Polymer Fiber

Parham Sadooghi, Cyrus Aghanajafi

K.N.T. University of Technology, Tehran, Iran

Received 13 April 2005; accepted 26 August 2005
DOI 10.1002/app.23665
Published online in Wiley InterScience (www.interscience.wiley.com).

ABSTRACT: Transient radiative and conductive heat transfer in a translucent medium with isotropic optical properties is investigated. The radiative two-flux equation is coupled with the transient energy equation and both equations are solved simultaneously. Transient solutions are obtained for a plane layer with refractive index equal to or larger than one, and with external convection and radiation at each boundary. Illustrative results obtained with the two-flux method show the effects of changing parameters such as optical thicknesses, refractive index, conduction–radiation parameter, and scattering on the transient temperature distribution within the layer. Results are given at different instances during the transient, and the distribution for the largest time is at or very close to steady state. © 2006 Wiley Periodicals, Inc. J Appl Polym Sci 101: 2277–2283, 2006

Key words: fiber; radiation; conducting polymers

INTRODUCTION

When a solid or stationary fluid is translucent, energy can be transferred internally by radiation in addition to heat conduction. Since radiant propagation is very rapid, it can provide energy within the material more quickly than diffusion by heat conduction. Radiation emitted in a hot material can also be distributed rapidly in the interior. The result is that transient temperature responses including radiation can be significantly different from those by conduction alone. This is important for evaluating the thermal performance of translucent materials that are at high elevated temperatures, are in high temperature surroundings, or are subjected to large incident radiation. Convective heating or cooling can also be applied at the boundaries. Radiant effects are accentuated as temperatures rise; it can be the temperature of material, the temperature of the surroundings, or both. Examples are heating a window by radiation emitted at high temperature from the sun, cooling a white hot ceramic by radiation loss to lower temperature surroundings,[1,2] heating an insulating shield during atmospheric reentry,[3,4] and heating translucent plastic with infrared lamps to soften it for manufacturing processes.

Interests in polymer fibers derived from synthetic organic polymers has grown substantially over the past 25 years. Underlying this growth is the remarkable range of mechanical properties exhibited by polymer fibers. Their properties may include high-temperature strength, high stiffness, low moisture absorption, no creep, or light weight. They are widely used in the chemical, metallurgical, food, and construction material industries as well as in the other branches of industry for the filtration of gaseous, aggressive liquid, and high-temperature substances. Their application in the electrical and electronic industries,[5–10] is especially important, because it has enabled a real increase in the reliability of electrical machines and the development of materials for IC's and microelectronics.

Radiation effects are studied less for transients than for steady state, because of the additional and computational complexities. Recently, they have attracted much more attention, and several excellent reviews on radiation and combined radiation and conduction energy transfer in dispersed media are available.[10–23]

This article presents an investigation of transient radiative and conductive heat transfer in a plane layer of polymer fiber, held at high temperature, and subjected to various radiative and thermal boundary conditions. It is accepted that the calculations of combined radiation and conduction heat transfer in rarefied diapered media may be carried out on the basis of using the radiation transfer equation in common with the energy conservation equation. For some types of thermal boundary conditions, the strict form of the radiation transfer equation is not used, and for simplification of calculation approximations are used. The most often used methods are approximate analytical methods. In this case, such as those developed from radia-

Correspondence to: P. Sadooghi parhampari2002@yahoo.com).

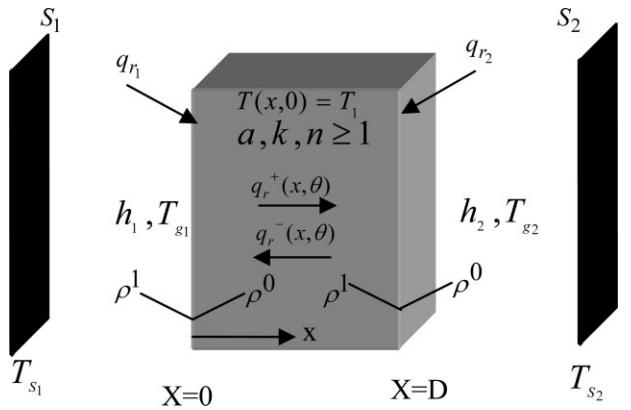

Figure 1 Geometry for transient radiation and conduction in a semitransparent layer of polymer fiber with isotropic scattering.

tive diffusion concepts, they do not yield accurate transient solutions as they cannot deal with the boundary conditions, and the differential approximation methods are accurate only for large optical thicknesses and fail at positions near the boundaries.

The solution of the exact radiative transfer equation is rather complicated, particularly, when the scattering is present: hence the best approach is the two-flux method. The two-flux method is used as a simplification for obtaining the radiative heat source term in the energy equation. For the general boundary conditions of external convection and radiation and for a layer with diffuse surfaces having unspecified temperatures, it has been demonstrated that the two-flux method predicts accurate transient and steady state temperatures and heat fluxes. The two-flux equations were examined as a mean for evaluating the radiative flux gradient in the transient energy equation. An advantage of the two-flux method is that isotropic scattering is included without any additional complication. The effect of variation of influence parameters, optical thicknesses, conduction–radiation parameter, and refractive index on the temperature distribution is considered carefully.

ANALYSIS

Energy and two-flux equations

A plane layer of polymer fiber, with thickness D (Fig. 1) is a heat conducting, gray emitting, absorbing, and isotropically scattering medium with $n \geq 1$, and its boundaries are assumed to diffuse. The layer is initially at uniform temperature T_i and is placed in surroundings so that each boundary receives radiative energy and is subject to convection. Transient temperature distributions are to be obtained in the layer until steady state is reached corresponding to the external radiation and convection conditions.

The transient energy equation in dimensionless form is as follows[24]:

$$\frac{\partial t}{\partial t^*} = N\frac{\partial^2 t}{\partial X^2} - \frac{1}{4}\frac{\partial \tilde{q}_r}{\partial X} \tag{1}$$

Properties are assumed independent of temperature. The gradient of the radiative flux $\partial \tilde{q}_r(X, t^*)/\partial X$ is obtained from the two-flux relation using the Milne-Eddington approximation[25–27]

$$\frac{\partial \tilde{q}r(X,t^*)}{\partial X} = \kappa_D(1-\Omega)[4n^2t^4(X,t^*) - \tilde{G}(X,t^*)] \tag{2}$$

where $\tilde{G}(X,t^*)$ is related to $\tilde{q},(X,t^*)$ by the equation

$$\frac{\partial \tilde{G}(X,t^*)}{\partial X} = -3\kappa_D\tilde{q}_r(X, t^*) \tag{3}$$

The $\tilde{q}_r$ and $\tilde{G}$ are related to the positive and negative radiative fluxes shown in Figure 1 by $\tilde{q}_r(X, t^*) = \tilde{q}_r^+(X,t^*) - \tilde{q}_r(X, t^*)$ and $\tilde{G}(X, t^*) = 2[\tilde{q}_r^+(X, t^*) + \tilde{q}_r(X, t^*)]$

BOUNDARY AND INITIAL CONDITIONS

The convective boundary conditions on the sides of the layer are as follows:

$$\frac{\partial t}{\partial X}\Big|_{x=0} = -\frac{H_1}{4N}[t_{g1} - t(0, t^*)] \tag{4a}$$

$$\frac{\partial t}{\partial X}\Big|_{x=1} = -\frac{H_2}{4N}[t(1, t^*) - t_{g2}] \tag{4b}$$

The radiative boundary conditions must now be specified including the effects of internal and external reflections at the surfaces. By considering the incident and reflected fluxes at an interface the following boundary relations between $\tilde{G}$ and $\tilde{q}_r$ were developed at each boundary[26]

$$\tilde{G}(0,t^*) = 4\frac{1-\rho^0}{1-\rho^i}\tilde{q}_{r1} - 2\frac{1+\rho^i}{1-\rho^i}\tilde{q}_r(0,t^*) \tag{5a}$$

$$\tilde{G}(1,t^*) = 4\frac{1-\rho^0}{1-\rho^i}\tilde{q}_{r2} + 2\frac{1+\rho^i}{1-\rho^i}\tilde{q}_r(1,t^*) \tag{5b}$$

To begin the transient solution of eq. (1), the specified initial condition, is a uniform temperature $T(x,0) = T_1$ so $t(X,0) = 1$. Initial distributions are also needed for $\tilde{q}_r(X,0)$ and $\tilde{G}(X,0)$. By differentiation, eqs. (2) and (3) can be combined to eliminate either $\tilde{q}_r(X,t^*)$ or $\tilde{G}(X,t^*)$ to give a second order equation for either of

these quantities. With $t = 1$ initially, these equations are solved analytically to give

$$\tilde{G}(X,0) = C_1 e^{\sqrt{B}X} + C_2 e^{\sqrt{B}X} + 4n^2 \quad (6a)$$

$$\tilde{q}_r(X,0) = -\frac{\sqrt{B}}{3\kappa_D}(C_1 e^{\sqrt{B}X} - C_2 e^{\sqrt{B}X}) \quad (6b)$$

where $B = 3\kappa_D^2(1 - \Omega)$. C_1 and C_2 are integration constants that are obtained by applying the boundary conditions (5a) and (5b) to eq. (6a). The following quantities are defined:

$$\alpha \equiv 1 - 2\frac{1+\rho^i}{1-\rho^i}\frac{\sqrt{B}}{3\kappa_D} \quad (7a)$$

$$\beta \equiv 1 + 2\frac{1+\rho^i}{1-\rho^i}\frac{\sqrt{B}}{3\kappa_D} \quad (7b)$$

$$\eta \equiv \beta e^{\sqrt{B}} \quad (7c)$$

$$\delta \equiv \alpha e^{\sqrt{B}} \quad (7d)$$

$$S_1 \equiv -4n^2 + 4\frac{1-\rho^o}{1-\rho^i}\tilde{q}_{r1} \quad (7e)$$

$$S_2 \equiv -4n^2 + 4\frac{1-\rho^0}{1-\rho^i}\tilde{q}_{r2} \quad (7f)$$

Then, the integration constants are as follows:

$$C_1 = \frac{-\beta S_2 + \delta S_1}{-\beta\gamma + \alpha\delta} \quad (8a)$$

$$C_2 = \frac{\alpha S_2 - \gamma S_1}{-\beta\gamma + \alpha\delta} \quad (8b)$$

NUMERICAL SOLUTION

Starting with the initial $t(X,0)$ and $\tilde{q}_r(X,0)$ relations, eq. (1) was integrated forward in time using the following explicit finite-difference algorithm at the interior grid points:

$$t(X,t^* + \Delta t^*) = t(X,t^*) + \frac{N\Delta t^*}{(\Delta X)^2}[t(X + \Delta X,t^*) - 2t(X,t^*) + t(X - \Delta X,t^*)] - \frac{\Delta t^*}{4}\frac{\partial \tilde{q}_r}{\partial X}\Big|_{\chi s^*} \quad (9)$$

The $t(t^* + \Delta t^*)$ at the boundaries were then evaluated using eqs. (4a) and (4b), with a three-point difference approximation for the temperature derivative

$$t(0,t^* + \Delta t^*) = \frac{\frac{H_1\Delta X}{2N}t_{g1} + 4t(\Delta X,t^* + \Delta t^*) - t(2\Delta X,t^* + \Delta t^*)}{3 + \frac{H_1\Delta X}{2N}} \quad (10a)$$

$$t(1,t^* + \Delta t^*) = \frac{\frac{H_2\Delta X}{2N} - t_{g2} + 4t(t - \Delta X,t^* + \Delta t^*) - t(1 - 2\Delta X,t^* + \Delta t^*)}{3 + \frac{H_2\Delta X}{2N}} \quad (10b)$$

After advancing t(X), each time increment the radiant flux gradient in the last term in eq. (9) must be advanced to $t^* + \Delta t^*$. This was done by solving eqs. (2) and (3) simultaneously for $\tilde{G}(X,t^* + \Delta t)$ and $\tilde{q}_r(X,t^* + \Delta t^*)$ using $t(X,t^* + \Delta t^*)$ on the right hand side of eq. (2). Then, $\partial\tilde{q}_r(X,t^* + \Delta t^*)/\partial X$ was evaluated from eq. (2). The simultaneous solution of eqs. (2) and (3) was obtained using a fourth-order Runge-Kutta method with a shooting procedure to satisfy the boundary conditions at $X = 0$ and 1. To begin the solution, the value of $\tilde{q}_r(X = 0)$ from the previous time step was used as an estimate, and the boundary condition eq. (5a) was solved for $\tilde{G}(X = 0)$. The solution was then obtained by Runge-Kutta integration from $X = 0$ to $X = 1$. The values of $\tilde{q}_r$ and $\tilde{G}$ obtained at $X = 1$ were checked to see if they satisfy the boundary condition in eq. (5b). Iteration was performed on $\tilde{q}_r(X = 0)$ until eq. (5b) was satisfied; the type of iterative method used is described in Ref. 26. The shooting method used here is convenient for absorption optical thicknesses, $aD \leq 8$. This two-point boundary value solution method becomes difficult when there is a large aD that causes the condition at the two boundaries to become less directly related. It is possible that other numerical techniques could partially eliminate this difficulty; a method using a Green's function is presently being developed. Using the $t(X)$ and $\tilde{G}(X)$, the radiant flux gradient was evaluated from eq. (2). The temperature distribution was then advanced to the next time increment using eqs. (9) and (10).

After checking various grid sizes, it was found that 41 evenly spaced points across the layer gave accurate solutions. Corresponding to this grid size ($\Delta X = 0.025$) and for $N = 0.1$ as used for the results given here. The Δt^* for a stable explicit calculation was estimated from the criterion for solving the transient heat conduction equation. The value Δt^* provided stable solutions for all of the results calculated here.

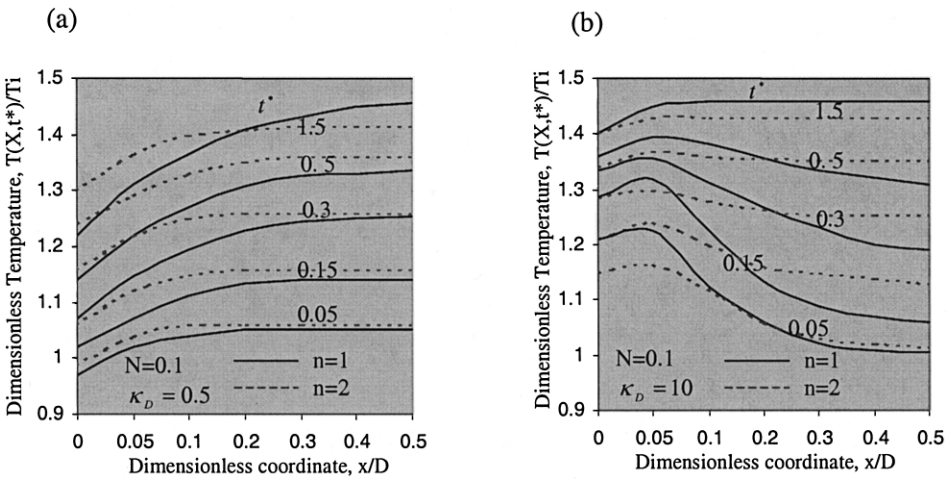

Figure 2 Effect of refractive index on transient temperature distribution in a layer initially at uniform temperature, after exposure to external radiation and convective cooling. Parameters: $N = 0.1, \tilde{q}_{r1} = \tilde{q}_{r2} = 1.5^4, H_1 = H_2 = 1, t_{g1} = t_{g2} = 0.5, n = 1$ and 2. (a) Optical thickness $\kappa_D = 0.5$; (b) optical thickness $\kappa_D = 10$.

RESULTS AND DISCUSSION

The transient temperature distributions given here start from a uniform initial temperature $T(X,0) = T_i$ so the $t(X,0) = 1$. For the results in Figure 2, the external radiation and convection conditions are symmetric on both sides of the layer so that the transient temperatures are symmetric and the distributions are given for one half of the layer. Results are given at five instances during the transient; the distribution for the largest time is at or very close to steady state. Figure 2 gives transient temperatures for a layer suddenly subjected on both sides to a higher temperature radiative environment so that $q_{r1} = \sigma T_{r1}^4 = q_{r2} = \sigma T_{r2}^4$ and to convective cooling. This could correspond to processing translucent plastics at elevated temperatures or by infrared heating. Figure 2(a,b) is for optical thicknesses $\kappa_D = 0.5$ and $\kappa_D = 10$. For $\kappa_D = 0.5$, the layer is somewhat optically thin and radiation can penetrate the entire layer, but there is significant absorption; this yields close to the maximum radiation effect throughout the layer. For $\kappa_D = 10$, the layer is somewhat optically thick and most absorption is near the boundaries. During the transient, the layer is heated on each side by black surroundings at a temperature 1.5 times the initial temperature ($\tilde{q}_{r1} = \tilde{q}_{r2} = 1.5^4$). Simultaneously, the layer is cooled by gas on each side at $T_{g1} = T_{g2} = 0.5T_i$. The $H_1 = H_2 = 1$ parameters are such that convection is somewhat comparable with radiation. There is moderate conduction as given by the parameter $N = 0.1$.

In Figure 2(a), where the layer is rather optically thin, external radiation passes into the interior to provide a fairly uniform internal heat source, some of which is removed by reradiation. Energy is removed near the wall by convection interacting with conduction. The result is that for small t^* the interior temperature remains fairly uniform. As t^* advances, the convection–conduction cooling penetrates the layer further and at the steady condition the profile has become somewhat parabolic as is typical for a layer with a uniform internal heat source. When the refractive index is increased from one to two, the temperature profiles are more uniform. This is a result of increased radiative energy transfer across the layer arising from internal reflections. It is noted that for small t^* the layer heats more rapidly when $n = 2$. This is caused by increased layer absorptivity for small κ_D.

The optical thickness is increased to $\kappa_D = 10$ in Figure 2(b). It is more difficult for radiation to pass into the layer interior. Absorption of incident radiation occurs in regions closer to the surface and the temperature increases strongly in the regions near the boundaries, for small t^*. Energy is transported into the interior by conduction and internal radiation, and the interior temperature distribution becomes uniform as steady state is approached. There is a very significant effect of refractive index; the profiles for $n = 2$ are much more uniform.

The results in Figure 3 demonstrate the effect on cooling a polymer layer of putting coatings on its boundaries so they are opaque and do not allow radiant transmission. It shows how coatings can be used to regulate heat transfer processes manufacturing with plastics. Equal convective cooling was provided at both surfaces. The solid lines are predicted temperatures when both internal radiation and conduction are included. These results are compared with the dot-dashed lines for internal heat conduction only.

The conduction–radiation parameter is on an attempt to characterize the radiative importance of conduction and radiation. In Figure 2(a), the $N = 0.05$ is small enough that there is a significant effect of internal radiation that makes the temperatures more uniform during

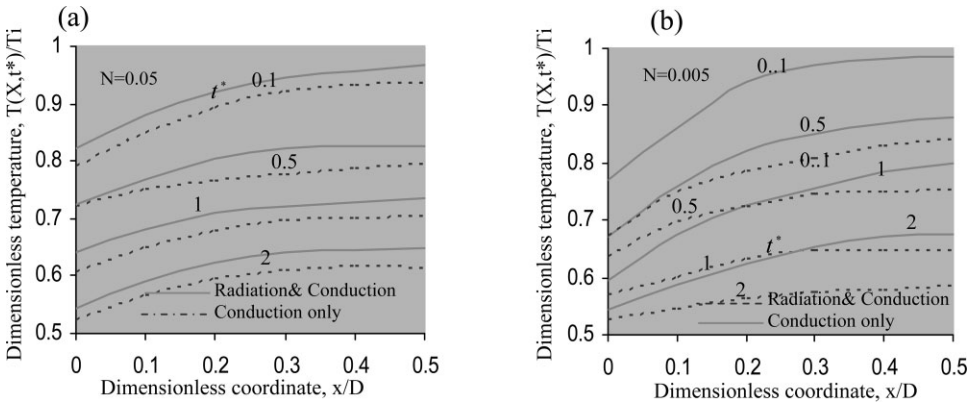

Figure 3 Transient temperature distributions for cooling a polymer layer, showing comparison of combined radiation–conduction with that for conduction only, $T_{g1} = T_{g2} = 1500\ K$, $h_1D/k = h_2D/k = 0.1$, (a) conduction–radiation parameter, $N = K/4Dn^2\sigma T_i^3 = 0.05$ and (b) conduction–radiation parameter, $N = K/4Dn^2\sigma T_i^3 = 0.005$.

transient cooling. The layer also cools more rapidly with combined radiation and conduction. In Figure 3(b), the conduction–radiation parameter is decreased to $N = 0.005$; therefore, there is less effect of conduction and the layer cools somewhat more slowly. Internal radiation makes the temperatures much more uniform than for conduction alone. More over radiative heating at a distance erases frontier gradients due to conduction and as a result very uniform temperature profiles are set up at long reduced times for the long times.

For Figure 4, the condition at the boundaries have been changed. The layer is heated on the hot side by a radiative flux equal to that from black surroundings at $T_{g1} = 1.5T_i$.

There is no convective cooling on the hot side, $H_1 = 0$. Cooling occurs on the cold side ($X = 1$) by convection with $H_2 = 1$ and $T_{g2} = 0.5T_i$ and by radiation to black surroundings at $T_{g2} = 0.5T_i$. The two parts of Figure 4 are for optical thicknesses 2 and 10. For Figure 4(a), the optical thickness, $\kappa_D = 2$, is such that maximum internal radiative are expected. At the hot side boundary, the lack of convective cooling provides a zero temperature gradient since radiation leaves from within the volume and not from the surface itself.

In Figure 4(b), the κ_D increased to 10 and there is more absorption of incident radiation near the boundary. Early in the transient there is a strong temperature rise near the hot boundary, while the temperatures decrease

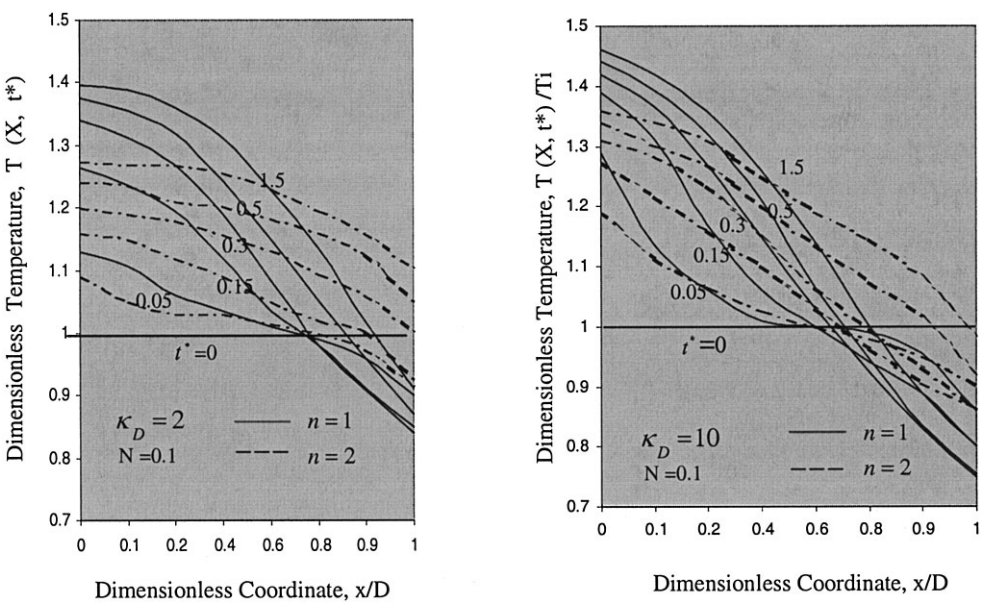

Figure 4 Effect of refractive index on transient temperature distributions in a polymer layer, initially at uniform temperature after exposure to external radiation on one side without convective cooling on that side; cooling is *b* radiation and convection at the other side. Parameters: $N = 0.1$, $\tilde{q}_{r1} = 1.5^4$, $t_{g2} = 0.5$,$H_1 = 0$,$H_2 = 1$, $t_{g2} = 0.5$, $n = 1$ and 2. (a) Optical thickness $\kappa_D = 2$; (b) optical thickness $\kappa_D = 10$.

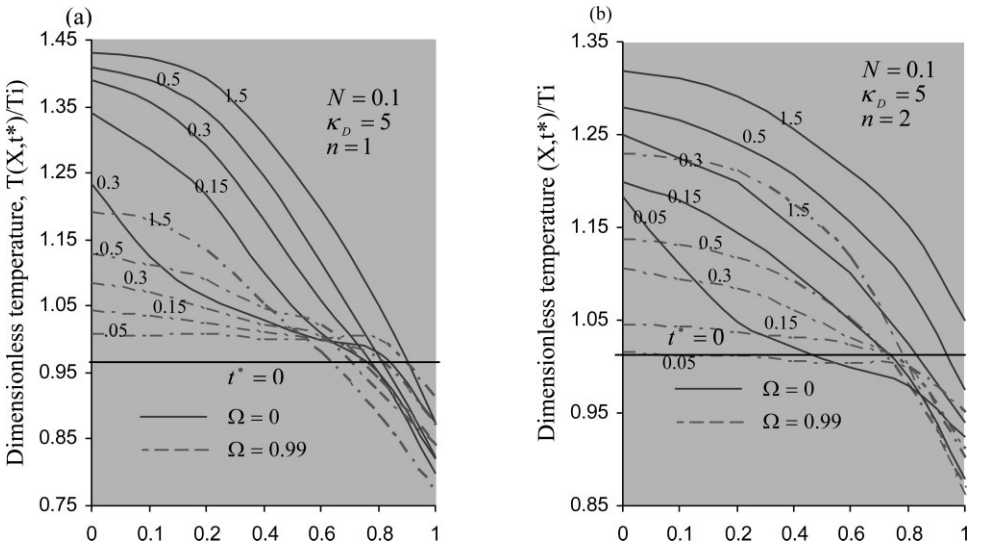

Figure 5 Effect of scattering on temperature distributions in a polymer layer initially at uniform temperature after exposure to radiation on one side and convective cooling on the other side. Parameters: $\kappa_D = 5, N = 0.1, \tilde{q}_{r1} = 1.5^4, \tilde{q}_{r2} = 0.5^4, H_1 = 0, H_2 = 1, t_{g2} = 0.5$. (a) Refractive index, $n = 1$; (b) refractive index, $n = 2$.

substantially at the boundary that is convectively cooled. Each part of the figure shows results for $n = 1$ and 2. Increasing n is not as effective in equalizing temperature as in Figure 4(a) because radiative transfer across the layer, as augmented by internal reflections is reduced by the increased κ_D. When $t^* = 1.5$ the temperature are within 7% of the steady state.

The effect of scattering is illustrated in Figure 5 for $n = 1$ and 2. The optical thickness is constant, $\kappa_D = 5$, and so an increase in scattering corresponds to a decrease in absorption.

The result is that the transient temperatures are decreased with increasing Ω. For $n = 2$ in Figure 5(b), the temperatures are somewhat more uniform than for $n = 1$ in Figure 5(a). [Note that the ordinate scales are different in Figs. 5(a) and 5(b)]. Compared with Figure 5(a), increasing Ω in Figure 5(b) does not have as large as effect in reducing the temperatures. For $n = 2$, the layer has internal reflections that make scattering more effective in augmenting absorption. For $\Omega = 0.99$, this makes the temperatures larger for $n = 2$ than for $n = 1$.

CONCLUSIONS

The two-flux method was used to obtain transient solutions for a plane layer of polymer, including internal reflection and scattering. Results for $n = 1$ and 2 show that the effect of the layer refractive index with boundary reflections assumed to diffuse. The layer was initially at uniform temperature, and different boundary conditions are examined.

First, it is placed in a hot radiative environment while being cooled by convection at both boundaries. The transient temperature distributions can have rapidly varying shapes when the optical thickness is large, and so the absorption of incident energy is concentrated near the boundaries. An important effect of refractive index is that internal reflections promote the distribution of radiative energy within the layer; this makes the transient temperature distribution more uniform. When the boundary conditions are changed and the layer is heated by radiation on one side and is cooled by convection and radiation on the other, the result shows that, if the optical thickness is less than about 10, internal reflections provided by refractive index of two have a substantial effect in equalizing the temperature distributions. Illustrative results obtained with this method demonstrate the effect of isotropic scattering coupled with changing the refractive index.

NOMENCLATURE

a	Absorption coefficient in layer (m^{-1})
B	The quantity, $3\kappa_n^2(1 - \Omega)$
c	Specific heat of radiating medium (J kg^{-1} K^{-1})
D	Thickness of semitransparent layer (m)
G	The flux quantity $2(q_r^- + q_r^-)$ (W m^{-2}): $\bar{G} - G\sigma T^1$
h_1, h_2	Convective heat transfer coefficients at $x = 0$ and D (W m^{-2} K^{-1})
H_1, H_2	Dimensionless parameters, $h_1/\sigma T_i^3$ and $h_2/\sigma T_i^3$
k	Thermal conductivity of layer (W m^{-1} K^{-1})
n	Refractive index of layer

N Conduction–radiation parameter, $k/4\sigma T_i^3 D$
q_r Radiative flux in the x-direction (W m^{-2}): $\tilde{q}_r = q_r/\sigma T_i^4$
q_{r1}, q_{r2} External radiation fluxes incident at $x = 0$ and D (W m^{-2})
$\tilde{q}_{r1}, \tilde{q}_{r2}$ Dimensionless radiation fluxes $q_{r1}/\sigma T_i^4, q_{r2}/T_i^4$
T Absolute temperature (K); $t = T/T_i$
T_{g1}, T_{g2} Gas temperatures for convection at $x = 0$ and D (K)
t_{g1}, t_{g2} Dimensionless gas temperatures, $T_{g1}/T_i, T_{g2}/T_i$
T_i Initial uniform temperature of layer (used as a reference T_i (K)
x Coordinate in direction across layer (m); $X = x/D$

Greek symbols

θ Time (s)
κ_D Optical thickness of layer, $(a + \sigma_s)D$
ρ Density of semitransparent medium (kg m^{-3})
ρ^i, ρ^0 Internal and external reflectivities at a boundary
σ Stefan-Boltzman constant (W m^{-2} K^{-4})
σ_s Scattering coefficient in layer (m^{-1})
t^* Dimensionless time, $(4\sigma T_i^3/\rho c D)\theta$
Ω Scattering albedo, $\sigma_s/(a + \sigma_s)$

References

1. Sadooghi, P.; Aghanajafi, C. Radiat Eff Defect Solid 2004, 159, 61.
2. Sadooghi, P. J Quant Spec Radia Transfer 2005, 92, 403.
3. Sadooghi, P.; Aghanajafi, C. J Fusion Energy 2004, 22, 59.
4. Sadooghi, P. J Quant Spec Radia Transfer 2005, 93, 461.
5. Sadooghi, P. J Reinfor Plast Comp 2005, 24, 1655.
6. Sadooghi, P. J Infra Phys Tech 2006, 47, 278.
7. Sadooghi, P. J Vin Add Tech 2005, 11, 28.
8. Macdiarmid, A. G.; Somasiri, N.; Wu, W. Mol Cryst Liq Cryst 1985, 121, 187.
9. Gurunathan, K.; Amalnerkar, D.; Trivedi, D. Mater Lett 2003, 57, 1642.
10. Heckner, K. H.; Kraft, A. Solid State Ionics 2002, 152, 899.
11. Scosati, B. Mater Sci Eng 1992, 12, 369.
12. Pant, R. P.; Dhawan, S.; Kataria, N.; Suri, D. J Magn Master 2002, 252, 16.
13. Saunders, C. B.; Lopata, V. J.; Kremers, W.; Chung, M.; Singh, A.; Kerluke, D. R. Radiat Phys Chem 1995, 46, 991.
14. Berejka, A. J.; Eberle, C. Radiat Phys Chem 2002, 63, 551.
15. Kerluke, D. R.; Cheng, S. Presented at the Proceeding of the 2nd Annual Automotive Composites Conference and Exposition of the Society of Plastics Engineers, San Francisco, May 2002.
16. Kaiser, P.; Astle, H. W. Bell Syst Tech J 1974, 53, 1021.
17. Reiss, H. Radiative Transfer in Nontransparent Dispersed Media; Springer: Berlin, 1988.
18. Viskanta, R.; Menguc, M. P. Appl Mech Rev 1988, 42, 241.
19. Reiss, H. High Temp-High Press, 1990, 22, 481.
20. Kaganer, M. G. Heat and Mass Transfer in Low Temperature Equipment; Energiya: Moscow, 1979; Chapter 2.
21. Reeves, H. M. J Mater Process Manuf Sci 2001, 9, 285.
22. Nasseri, S.; Tanner, R.; Department of Mechanical Engineering, Optical Fiber Tech. Center, University of Sydney, Internal report, 2001.
23. Sucbei, M. Presented at the Proceedings of the Plastic Optical Fibers Conference, Vrije. University, Amsterdam, 2001.
24. Siegel, R.; Howell, J. R. Thermal Radiation Heat Transfer, 3rd ed.; Hemisphere: Washington, DC, 1992.
25. Sidalle, R. G. In Proceeding of the Fourth Symposium on Flames and Industry, Imperial College, London, UK. The Institute of Fuel, 1972; p 16169.
26. Siegel, R.; Spuckler, C. M. Int J Heat Mass Transfer 1994, 37, 403.
27. Press, W. H.; Flannery, B. P.; Teukolsky, S. A.; Vetterling, W. T. Numerical Recipes (FORTRAN Version), 582–585; Cambridge University Press: Cambridge, UK, 1989.